Astron. Astrophys. 246, 481–489 (1991)

ASTRONOMY AND ASTROPHYSICS

Asphericity effects in scattering dominated photospheres

P. Höflich

Max-Planck-Institut für Physik und Astrophysik, Institut für Astrophysik, Karl-Schwarzschild-Strasse 1, D-W-8046 Garching, Federal Republic of Germany

Received August 3, accepted November 24, 1990

Abstract. Monte Carlo calculations for axial symmetric, scattering dominated photospheres have been performed in order to study systematically the effects due to the direction dependent luminosity and to reinvestigate the continuum polarization in SN 1987A (Mendez et al. 1988). We found that the optical depth and the occultation effects are important for the interpretation of the observed polarization, and that the differences between the electron and the density profile are substantial for the understanding of the observed time dependence of the linear polarization in SN 1987A. The observed polarization can be well understood by prolate or oblate ellipsoids ($a/b = 0.9$ or 1.2) if SN 1987A is seen at an inclination angle of less than 56° with a most probable value of about 40°.

Key words: radiation transport – electron scattering – polarization – direction dependent luminosity – SN 1987A

1. Introduction

The investigation of the emitted light of Type II supernovae (SN II) is important for various fields in astronomy and astrophysics. The observed spectrum gives direct information on the physical and chemical conditions of the supernova photosphere at a given time. Deeper layers of the expanding envelope are observable at later times. Therefore, a detailed spectral analysis of the time evolution is helpful in order to answer questions concerning the overall structure of the envelope. In principle, this allows for an investigation of the explosion mechanism of SN II, for the test of hydrodynamic models and of the final stages of the evolution of massive stars. In particular, supernova 1987A in the Large Magellanic Cloud (LMC) has triggered a rapid development of tools for atmospheric diagnostics of SN II, because it has provided a lot of information due to the complete sample of observations. The power of a spectral analysis has been demonstrated by sophisticated models which take extention and NLTE effects into account. For recent reviews on SN 1987A see Arnett et al. (1989) and Hillebrandt & Höflich (1989). Unfortunately, the spectra hardly provide any direct information on the geometrical structure of the envelope, i.e. the spectral analysis is insensitive to an important photospheric property which may give essential hints for our understanding of supernova explosions.

However, the emitted photons contain information about the geometry due to their polarization. In principle, a "consistent" photospheric analysis also has to take these data into account.

Moreover, deviations from sphericity may also result in a direction dependence of the emitted flux, and consequently may effect the bolometric light curves (LC) of SN II as determined from the observations.

So far, polarization measurements of SN II are available only in the case of SN 1987A. Fortunately, the rapid evolution of the instrumentation will allow for further polarization observations of supernovae other than SN 1987A. Therefore, it may be helpful to investigate the phases of the expansion during which an envelope shows the highest linear polarization for a given asphericity.

During the first few months several groups have observed frequency dependent linear polarizations of up to about 0.5% in the continua as well as in lines of SN 1987A (Barrett 1987; Colchiatti et al. 1988; Mendez et al. 1988; Schwarz & Mundt 1987; Schwarz 1987). Jeffry (1987) was the first to derive from the polarization data of the Balmer lines an axis ratio E of the order of about 0.6 to 0.8 assuming an oblate ellipsoid. For the same geometry, Mendez et al. (1988) derived somewhat larger values from the continuum data. In this analysis, time dependent photospheric radii and exponential density slopes are taken which are indicated by Woosley's model 10H (Woosley 1988). Mendez et al. were successful in determining the degree of polarization at a certain time and they were able to reproduce its time dependence over the first 40 days. From these data they derived an ellipticity of the order of 0.8 to 0.92 seen at an inclination of less than 15°, i.e. the envelope is seen nearly equator on. They used the analytical formulae given by Cassinelli et al. (1987), i.e. they included the depolarization factor due to the extension of the central source but applied the optically thin approximation according to Brown & McLean (1977) which also neglects the occultation of the central source. By assuming a constant mass of the photon emitting region, Mendez et al. (1988) explained the decline of the polarization as being due to a shrinking of the scattering optical depth at the photosphere. The decrease of the optical depth is caused by the decrease of the density slope as inferred from hydrodynamical calculations (Woosley et al. 1987).

Höflich et al. (1989) have criticized this approach by arguing that the influence of optical depth effects may be important. Then, the relation between the size of the polarization and the

Thomson optical depth would not hold any more. In contrast, the polarization depends weakly on the optical depth if the continuum forming region is dominated by electron scattering (see below). For SN 1987A, the continuum forming region is totally scattering dominated, i.e. τ_{sc} is larger than 1 during the photospheric phase. This can be inferred from the spectral analysis by NLTE models (Höflich 1988ab), from the observed colours (e.g. Catchpole et al. 1987) and also from the photospheric properties obtained from light-curve models if the ionization equilibrium is calculated by the Saha equation (e.g. of Shigeyama et al. 1988). For that reason a reduction of τ can hardly explain the observed time dependence of the linear polarization. Furthermore, the slope of the electron and particle density profiles differ significantly after the recombination phase which is encountered by SN 1987A already one to two weeks after the explosion (Höflich 1990a). Similar problems occur if the polarization of a line is investigated and the radial dependency of the line opacity and of the source function is identified with the slope of the density profiles (Jeffry 1987). For the lines the problems may be even more severe than for the continua because deviations from the local thermodynamical equillibrium have to be taken into account which may depend not only on the radial distance but on the angular coordinates. Therefore, Höflich et al. (1989) restricted their analysis to the continuum problem by using a Monte Carlo method which easily allows for taking the optical depth, occultation and etc. effects into account. The observed size of the polarization and its time dependence durng the first 50 days can be reproduced by an oblate ellipsoid with an axis ratio in the order of about 0.94 and an inclination angle of 0° as a result of the increasing depolarization due to the extension of the central source. However, a spherical inner boundary was used in this investigation. This may be regarded as in disagreement with the assumption of a time independent flattening of the entire envelope. Additionally, this flattening must be regarded as a lower limit only because no information besides the frequency independent information entered the analysis.

The differences discussed earlier reflect partially the way the problem was treated and the large number of free parameters. Another reason for the discrepancies may be that the geometry of the regions differ which are measured by the lines and the continua, respectively. But both spectral features are dominated by hydrogen and it is hard to understand how its distribution can be altered significantly. Another explanation may be connected with the problem of the relation between the density profile and the line source functions (see above). Because of these problems for the interpretation of lines we restrict our investigation again to the continua during the phases of Thomson scattering domination.

In a first part we will discuss the numerical methods used, the physical assumptions and the free parameters of the models.

One of the main problems is the large number of free parameters relative to the information available from the measurements. Therefore, we study the sensitivity of the detectable quantities on the basic parameters for some cases in a systematic way, and we investigate the additional information which can be gained by the direction dependence of the bolometric luminosity. This may be interesting not just regarding SN 1987A and other supernova but more generally scattering dominated photospheres such as novae, WR stars etc. We neither want to discuss parameter sets which can be better investigated by analytical investigations for the optically thin regime (e.g. Brown & McLean 1977; Cassinelli et al. 1987) nor those parameter ranges which have been investigated already by a Monte Carlo technique for situations which are dissimilar from supernovae envelopes. The investigation of Daniel (1982) may stand as an example who has assumed a point like source and a constant density envelope.

Finally, our models are applied to SN 1987A. The observed polarization is reinvestigated and discussed in more detail than in the earlier work (Höflich et al. 1989). In particular, we will not restrict our discussion on oblate ellipsoids and we will include also additional information on the assymetries which can be gained by the observed light curve.

2. A Monte Carlo method for the calculation of the polarization

During the last few years several groups have derived analytical solutions for the polarization problem under certain assumptions like the optical thin limit for point like sources, or even extended sources (e.g. Brown & McLean 1977; Cassinelli et al. 1987). Unfortunately, these methods are inadequate for the optical thick supernovae atmospheres with thermalization optical depths of about 2 in Thomson scattering (Höflich 1987ab, 1990). Here, we use a newly developed Monte Carlo code similar to one which has been developed by Daniel (1982) for point like sources, but which has been generalized to overcome the restriction imposed on the central boundary and on the density slope. An advantage of Monte Carlo methods is the high flexibility with respect to the geometry (in fact it is simple to generalize for fully 3 dimensional geometries), and it is easy to build up a computer code. Its disadvantage as compared to a direct solution of the radiation transport equation is the larger amount of computer time needed. In particular, the integration along the rays is extremely time consuming if it is performed numerically. Thus, one trivial but still interesting feature of this code may be the option that all the time consuming integrations can be performed by analytical expressions for appropriate density distributions. Furthermore, we restrict the use to continuum problems only. Both advantages and disadvantages of the MC method are connected because no information is taken into account about the mathematical structure of the radiation transport equation.

Our code has been developed to calculate the continuum polarization for different geometries (Höflich & Zorec 1989; Höflich et al. 1989). Results of our test calculations have been compared to those of Daniel (1982) in the whole parameter space and also to the analytical solutions of Brown & McLean (1977). We found good agreement in all cases within the statistical errors which are expected from the finite number of photons used.

Here, the angular space of the emitted photons is discretized by 30 to 60 counters. The calculations are stopped if at least 500 000 to 3 000 000 test particles per detector are counted for the general investigation and for the application to SN 1987A, respectively, to get a reasonable signal to noise ratio ($\lesssim 5\%$). Because the polarization is defined as the difference between two intensities with orthogonal electrical vectors, the numerical noise of the polarization data declines with its relative size.

The theory of polarization and the Stoke's formalism are described very well in the first edition of the book of Van den Hulst (1957). There, the problem is discussed as a solution of the differential equation. For the Monte Carlo method one has just to transfer the equations into a particle picture. Here, we want to point out the basic relations only which we have used.

For the transformation into the particle picture, the intensity I can be divided in a sum of the two components which are normalized so that

$$I = I_r + I_l = P_r^2 + P_l^2 = 1. \tag{1}$$

P_r and P_l are the electrical components of the field. The linear polarization is defined by

$$\mathscr{P} := \frac{(I_l - I_r)}{(I_l + I_r)}. \tag{2}$$

In the particle "picture" the radiation transport of polarized light can be well described by the travel of a photon which is characterized by the polarization vector $\underline{P}$ and the orthogonal direction $\underline{D}$, i.e.

$$\underline{P} := \{P_x, P_y, P_z\}$$
$$\underline{D} := \{D_x, D_y, D_z\} \tag{3}$$

where

$$\|\underline{P}\| = \|\underline{D}\| = 1 \tag{4}$$

and

$$\underline{P}\,\underline{D} = 0. \tag{5}$$

Initially, a number of photons are emitted at the inner edge of the configuration. The directions are either given by assuming a locally isotropic radiation field (random emission in all directions), or, alternatively, by a disk of locally constant brightness, i.e. the number of emitted photons is $\propto \cos\theta$ where θ is the angle between the vector orthogonal to the surface and the direction of the emitted photon. These are different cases because the boundary condition has some influence on the number of multiple scattering processes, in particular, in the case of optically thin envelopes.

Each photon travels a certain distance λ which is given by

$$\lambda = -\frac{1}{\chi\rho} \ln \mathscr{R} \tag{6}$$

where $\mathscr{R}$ is a random number with $\mathscr{R}\varepsilon[0, 1)$. χ and ρ are the opacity and density,respectively.

After the distance λ the photon is scattered and the new direction has to be specified. After some simple geometrical considerations, we end up with the following equations

$$\mathscr{R}_1 = \frac{\varphi_\alpha}{2\pi}; \quad \mathscr{R}_2 = \sin^2\alpha \tag{7}$$

where

$$\mathscr{R}_{1,2} \in [0, 1). \tag{8}$$

ϕ_α and α are the Eulerian angles of the new direction in the system of the old direction. We define $\underline{q} = \{q_x, q_y, q_z\}$ by

$$\underline{q} := \underline{P} \times \underline{D}. \tag{9}$$

The relations together with $\mathscr{R}_{1,2}$

$$\underline{q}\,\underline{D} = \underline{q}\,\underline{P} = \underline{D}\,\underline{P} = 0 \tag{10}$$

result in the transformation relations

$$\underline{D}_{\text{new}}\,\underline{P} = \cos\alpha = h_p$$
$$\underline{D}_{\text{new}}\,\underline{q} = \sin\alpha\cos\varphi_\tau = h_q$$
$$\underline{D}_{\text{new}}\,\underline{D} = \sin\alpha\sin\varphi_\alpha = h_D. \tag{11}$$

The sign of $\sin\alpha$ has to be specified randomly to end up with a function for the transformation. The new direction D_{new} is calculated by the equation

$$\underline{D}_{\text{new}} = h_p\underline{P} + h_q\underline{q} + h_D\underline{D}. \tag{12}$$

When a photon has left the envelope, a direction Θ is defined as the angle between its direction and the symmetry axis. Its linear polarization is expressed by

$$\mathscr{P}(\theta) := (2P_z^2(\theta)/\sin^2\theta - 1).\frac{\sin\theta}{\theta}. \tag{13}$$

Finally, the total polarization is calculated by superposing the photons which are emitted into a certain direction.

Here, pure Thomson scattering atmospheres are assumed. This is a reasonable assumption since the continuum opacities of SN II are dominated by electron scattering. The light becomes unpolarized at large optical depths both by thermalization processes and by multiple scattering. Hence, the light is taken as unpolarized at the inner core of the maximum optical depth $\tau_{\max}$. A photon is assumed to be thermalized if it passes the core, i.e. it is absorbed and re-emitted "unpolarized". The geometrical structure of this boundary was taken as spherically symmetric or, alternatively, as given by an ellipsoid of the same shape as the envelope. The first case corresponds to a geometrically undisturbed interior, while the second case is valid if the isotropic radiation field is formed in a homologous expanding elliptical envelope in which the depolarization is produced by thermalization processes i.e. by collisional processes. Constant surface brightness (CS) or global isotropic emission (IE) are adopted. These cases are dissimilar for all boundaries but spherical ones. Power law density profiles are taken with a cut off at a certain surface. This boundary corresponds to the recombination radius of H, and it should not be regarded as a numerical artifact but as a physical parameter.

In summary, we keep the following parameters free:

(a) the maximum optical depth $\tau_{\max}$ of inner edge,

(b) the density slope which is described by the power law index n ($r \propto r^{-n}$),

(c) the extension ε of the inner boundary relatively to the equatorial radius,

(d) the axis ratios of A/B of the elliptical density distribution of the envelope,

(e) the geometry of the inner core and

(f) the global and local emission which is assumed at the inner boundary.

3. Dependency of the observable quantities on the model parameters

In this section we study the relations between detectable quantities and the free parameters of our model with one basic set. They are given by

(a) $\tau_{\max} = 1$,

(b) $r \propto r^{-2}$,

(c) $\varepsilon = 0.01$,

(d) $E = A/B = 0.5$ and

(e) the core is spherically.

All variables are kept fixed except of the one under investigation (see Figs. 1–7). We use this basic set because it allows for a discussion of all the effects relevant for atmospheres of SN II

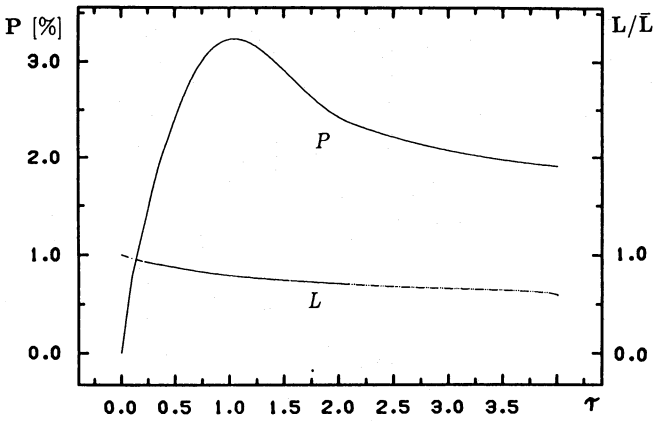

Fig. 1. Linear polarization (P) and the normalized flux (L) as a function of the maximum optical depth τ for an oblate ellipsoid [$N(r) \propto r^{-2}$; $\varepsilon = 0.01$; $E = 0.5$; spherical inner boundary, $i = 90°$]

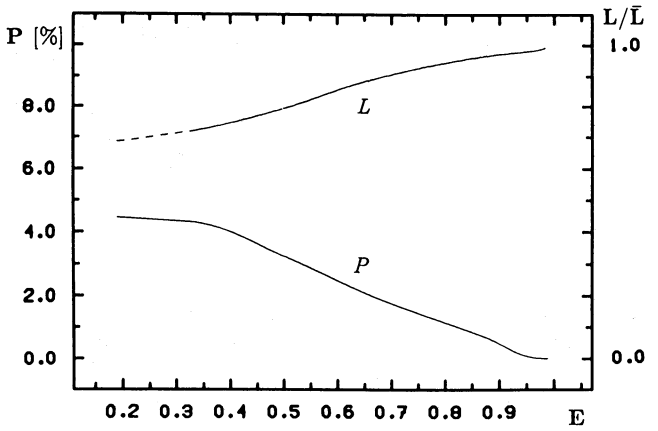

Fig. 4. Linear polarization (P) and the normalized flux (L) as a function of the fattening E for an oblate ellipsoid [$\tau_{max} = 1$; $N(r) \propto r^{-2}$; $\varepsilon = 0.01$; spherical inner boundary; $i = 90°$]

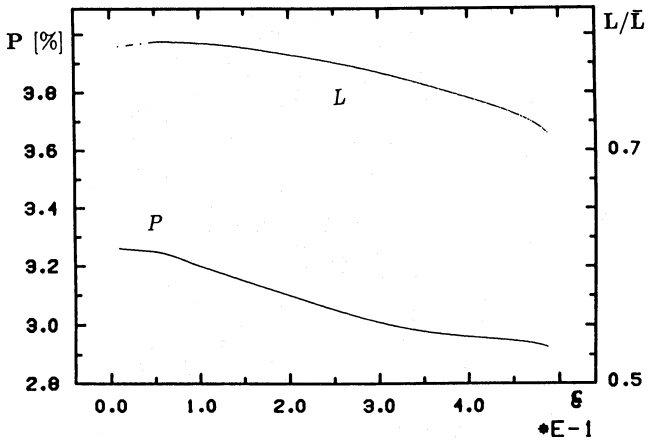

Fig. 2. Linear polarization (P) and the normalized flux (L) as a function of the extension ε for an oblate ellipsoid [$\tau_{max} = 1$; $N(r) \propto r^{-2}$; $E = 0.5$; spherical inner boundary; $i = 90°$]

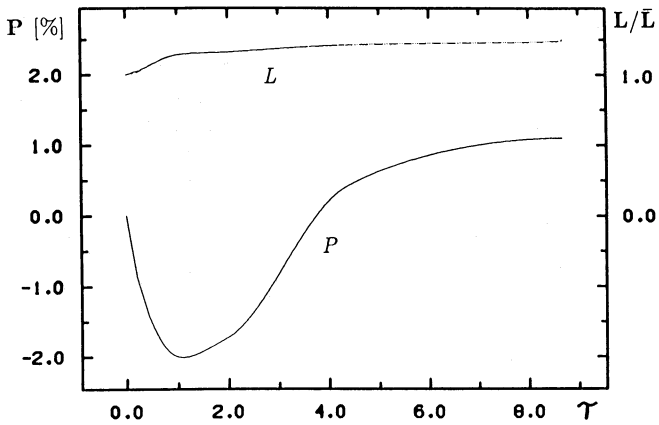

Fig. 5. Linear polarization (P) and the normalized flux (L) as a function of τ_{max} for a prolate ellipsoid [$N(r) \propto r^{-2}$; $\varepsilon = 0.01$; $E = 0.5$; spherical inner boundary; $i = 90°$]

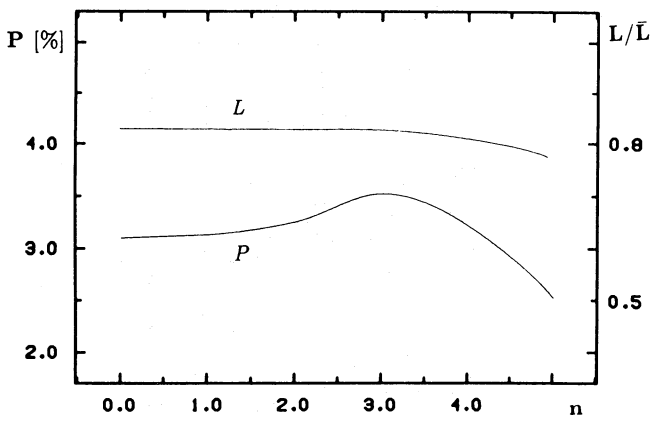

Fig. 3. Linear polarization (P) and the normalized flux (L) as a function of the exponent n of the density slope for an oblate ellipsoid [$\tau_{max} = 1$; $\varepsilon = 0.01$; $E = 0.5$; spherical inner boundary; $i = 90°$]

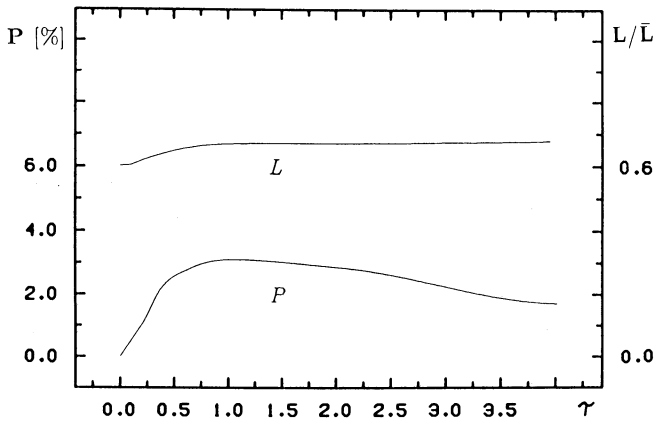

Fig. 6. Linear polarization (P) and the normalized flux (L) as a function of τ_{max} for an oblate ellipsoid [$\tau_{max} = 1$; $N(r) \propto r^{-2}$; $\varepsilon = 0.01$; $E = 0.5$; elliptical inner boundary; isotropic emission; $i = 90°$]

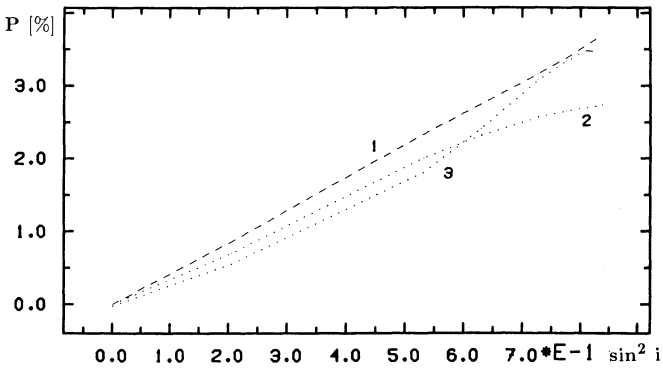

Fig. 7. Linear polarization as a function of the inclination i of the observer for an oblate ellipsoids with a spherical (*1*) and an ellipsoidal (*2*) core. In addition, the relation for a prolate ellipsoid is given (*3*) [$\tau_{max}=1$; $N(r)\propto r^{-2}$; $\varepsilon=0.01$; $E=0.5$]

and it corresponds approximately to the later stages of SN 1987A. The axis ratio E was chosen since it was suggested for SN 1987A (Jeffry 1987) and it saves computer time without changing the general trends (see above).

First, oblate ellipsoids with a spherical inner core are studied (Figs. 1–3, 5) that are seen equator on (inclination $i=90°$). Constant surface brightness is assumed as the condition for the local emission, i.e. a disk of constant brightness would be observed if the scattering envelope would be removed. All graphs are constructed on the basis of 8–12 models each.

The polarization is produced by the change of the direction of the electrical field vector by Thomson scattering. For this reason, it raises linearly with the optical depth as long as the number of interactions is small, i.e. in the optical thin limit. This assumption breaks down already at optical depths of the order of 0.2 to 0.3 owing to multiple scattering processes which result in a depolarization as a consequence of the reduced information on the global geometry. In addition, this effect is responsible for the global maximum at value of τ of about 1 . . . 1.5. This can be regarded as a typical optical depth of the maximum polarization produced by an arbitrary oblate ellipsoid (for a comparison see Daniel 1982). Therefore, the size of the polarization can be used effectively to derive a lower limit for deviations from sphericity.

An increasing relative core radius has similar consequences as multiple scattering (Fig. 2). It reduces the correlation of the initial directions of photons and results in a covering of photons with a certain direction due to the finite core size. Hence, the polarization decreases with increasing core size. The relation of Cassinelli et al. (1987) holds up to $\tau\approx 1$ if the occultation remains small, although the depolarization is derived for the optically thin limit because only the total number of photons enters. Note that the depolarization due to the extension of the photosphere becomes important in the recombination phase of type II supernovae owing to the extension of the photosphere which becomes comparable with the H II region (see Höflich 1990, Chap. IV–V).

Steeper density slopes reduce the probability of multiple scattering of a photon without being thermalized at the inner edge (Fig. 3). Consequently, the polarization firstly grows with n. Additionally, there is a counteracting mechanism. The depolarization caused by the extension of central source increases because most of the photons are scattered near the emitting source for large n. Therefore, the polarization decreases finally with n.

As has been demonstrated above, the size of the linear polarization depends mainly on the influence of the non-local curvature in the distribution of the scattering particles. Consequently, the polarization varies strongly with the axis ratio E. The dependence of the polarization is shown in Fig. 4 for our parameter set.

From the considerations given above one might conclude that the optically thin approximation can be regarded as a good first guess to determine deviations from sphericity. This is incorrect, in general (Fig. 5). For example let us consider the polarization as a function of τ_{max} for prolate ellipsoids with same basic set. The polarization differs from those of an oblate ellipsoid (see Fig. 1 for comparison) in size, general dependency and angle dependency as soon as optical depth effects become important. Here, the size of the total polarization depends on τ_{max} even for the optically thick case for $\tau\geq 3$ in contrast to oblate density distributions.

Finally, the influence of the geometry of the inner edge shall be considered in some detail assuming a constant surface brightness of the core. The dependencies (Fig. 6) look similar than for the case of spherical boundary conditions. However, the equatorial polarization is smaller and the maximum is less pronounced than for spherical boundaries (Fig. 1) because of the increasing probability for multiple scattering processes. One should be aware, however, that strong depolarization and occultation effects can occur for less extended scattering regions (see next section).

In Fig. 7 the calculated polarization with the basic set of parameters set is shown as a function of the inclination angle i. The correlation between the inclination angle and the size of the linear polarization can be approximated by a $\sin^2 i$ function as was derived by Brown & McLean (1977) for an arbitrary axisymmetric situation if an isotropic central emission was adopted. The deviations correspond to about an uncertainty of the order of 0.1 in $\sin i$ for oblate ellipsoids. However, in this specific case the prolate ellipsoid shows its maximum polarization when it is seen from more polar directions.

One should note that a non-spherically inner boundary implies a non-isotropic radiation field, i.e. an oblate ellipsoid emits more photons in the polar than in the equatorial direction. This leads us to the question of determining the bolometric luminosity in non-spherically configurations if the optical depth becomes significant. The influence of the different parameters are also shown in the Figs. 1–6. The change of the direction dependence of the luminosity mostly depends on the flattening E and the maximum optical depths which both reflect the dependence on the direction dependent total escape probability. The correlation of the direction dependence of the luminosity and the polarization depends on the geometrical structure of the envelope and the core if a constant surface brightness is assumed (see Figs. 1 and 6). For the prolate ellipsoid (Fig. 5) the equatorial luminosity is enhanced by up to 30% and stays constant for increasing τ_{max}, whereas the total polarization changes between its extremes, i.e. the polarization may change its sign in contrast to oblate ellipsoids. Thus, different geometries may be distinguished, in principle, if the bolometric LC is well known from theoretical models.

We can conclude from the discussions given above that the variation of the polarization and the direction dependent luminosity can be understood as a result of the correlation between the

emitted photons and the global information about the geometry. Therefore, the free variables may cause similar variations. Furthermore, the relations between the free parameters and the observable quantities are not monotonic as in the optically thin limit and the same size of polarization can be produced even if just one parameter is altered. A reduction of the parameter space is essential for the interpretation. For instance this can be done effectively by using data from a spectral analysis since it may fix the free parameters (a) to (c) (see above).

4. Application to SN 1987A

In order to compare the predicted and observed polarization of SN 1987A, the contribution of the interstellar matter (ISM) has to be separated. The light of stars is unpolarized, in general, and the measured polarization can be attributed to the ISM. The interstellar polarization of the visual light ($\lambda_{max} = 5400$ Å) in the direction of Sk − 69°202 was determined to be about 0.41% (Schmidt 1976; region VIII) on the basis of a number of bright stars in the LMC for the region of Sk − 69°202. According to studies of the LMC region, the interstellar polarization of both the Galaxy and the LMC behave normally (Clayton et al. 1983; Schmidt 1976). Therefore, the frequency relation of Serkowski et al. (1975) can be used to compare different sets of data. Unfortunately, the interstellar polarization shows variations up to 0.3% in this region. Hence, a specific star close to SN 1987A may give a better estimate. A linear polarization of about 0.5% was derived at a position angle of 44° for the nearby star Sk − 69°203 (Mendez et al. 1988). The constant position angle of the residual polarization (27°) should be regarded as a hint that the local contribution of the ISM near SN 1987A is small (Mendez et al. 1988). Nevertheless, the small scale density fluctuations of the ISM in the surroundings of SN 1987A should be kept in mind that were found by high resolution imaging (Wampler et al. 1990). In the following we attribute the residual polarization completely to the expanding envelope (Figs. 8–10) and we assume that the ISM is unaffected by SN 1987A. An error in the interstellar polarization results in a shift of all observations by a constant value, only. Further uncertainties are due to the scatter of the measurements of the order of about 0.1%.

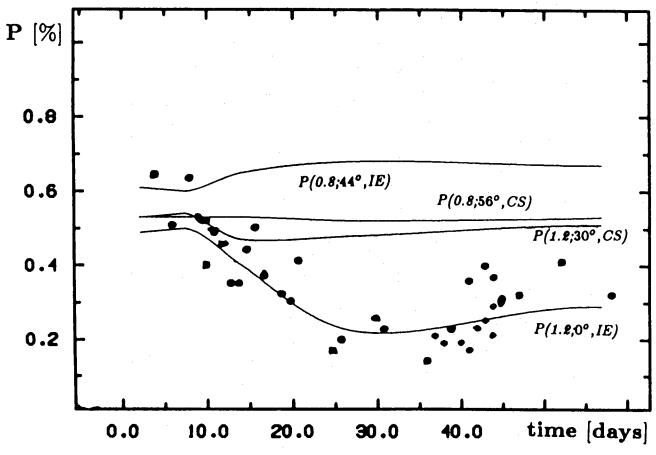

Fig. 8. Linear polarization for different configurations as identified by the vectors (E, i, boundary condition) as a function of time since the explosion of SN 1987A. The mass density slope is identified with the electron density slope ($\tau_{max} = 2$; see Table 1 for all other parameters). The *dots* mark the measured data of SN 1987A (Mendez et al. 1988)

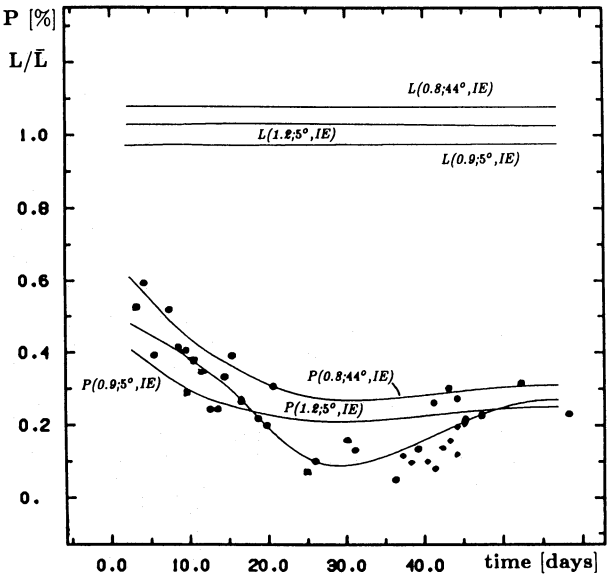

Fig. 9. Linear polarization for different configurations as identified by the vectors (E, i, boundary condition) as a function of time since the explosion of SN 1987A. The electron density profile is used. Isotropic emission is assumed at the inner boundary ($\tau_{max} = 2$; see Table 1 for all other parameters). The *dots* mark observations of SN 1987A (Mendez et al. 1988)

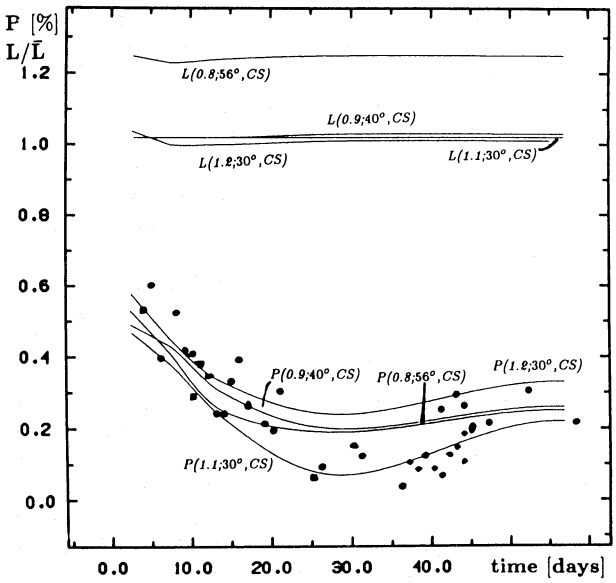

Fig. 10. Linear polarization for different configurations as identified by the vectors (E, i, boundary condition) as a function of time since the explosion of SN 1987A. The electron density profile is used. Constant surface brightness is taken as the inner boundary ($\tau_{max} = 2$; see Table 1 for all other parameters). The *dots* mark observations of SN 1987A (Mendez et al. 1988)

As demonstrated in the previous section, the number of free parameters is very large and, thus, they cannot be deduced simultaneously just from the observed polarization. On the other hand, several properties of the photosphere are known from the

spectral analysis (see table). These can be kept fixed provided that the deviation from sphericity of the continuum forming region remains small. The core radius can be deduced from the photospheric radius and its density. We take the recombination radius $R_{\mathrm{H\,II}}$ of H as the outer boundary and the exponent $\tilde{n}$ as the slope of a power law for the electron distribution. Furthermore, we adopt an ellipsoidal geometry of the core in contrast to the earlier investigation (Höflich et al. 1989) because for SN II envelopes this approximation is more realistic than a sphere (see above).

The thermalization optical depth is of the order 1.5 to 2.5 in all our photospheres of SN 1987A (Höflich 1988ab, 1990ab). The polarization is slowly varying in this τ range in comparison to the uncertainties implied by the other free parameters. In addition, local fluctuations in the electron density may cause some error with respect to the "real" thermalization optical depth. Therefore, for the sake of simplicity we take the optical depth $\tau_{\max}=2$ as a standard value. The radiation field at optical depths of 2 can be regarded as locally isotropic and, therefore, we use the condition of local isotropic emission at the inner boundary.

Unfortunately, little is known about the global deviations from sphericity of SN II neither from hydrodynamical models nor from the observations. One may argue that the progenitor of SN 1987A was a rapidly rotating star on the main sequence (Weiss et al. 1988) of the spectral class O, and an oblate ellipsoid may be the most probable configuration (Jeffry 1987; Mendez et al. 1988). However, the maximum possible rotational energy of the progenitor ($\leq 10^{50}$ erg) is much less than the explosion energy ($\approx 1.3\,10^{51}$ erg, Höflich 1990; Höflich et al. 1990). Therefore, in general, the density shape of the initial stellar configuration cannot be sustained during the explosion because of the energy and angular moment conservation. Depending on the initial conditions, the shock wave can pass the polar directions more rapidly than the equatorial area and a flattened stellar core may result in an axial elongated geometry of the envelope. Anticipating that the initial stellar rotation of the progenitor causes the deformation, an axial symmetry is somehow favorable. The question whether this would result into an oblate or prolate structure is still an open question (e.g. Symbalisty 1984; Yamada & Sato 1990). We have used prolate as well as oblate ellipsoids as the two examples for axi-symmetric configurations. Since the global geometry most likely is unchanged after the homologous phase is entered (Fryxell et al. 1989; Shigeyama et al. 1988; Woosley et al. 1988) the axis ratio of the geometrical structure does not depend on the time. However, if the initial stellar rotation did not cause the asymmetries, there is no strong reason to assume any rotational symmetry other than for the sake of simplicity.

Here, we use atmospheric parameters which allow for a good representation of the spectra by NLTE models (Höflich 1988ab). The density structure as derived by several hydrodynamical models are very similar for SN 1987A (see table; Höflich 1990b, Chap. II) and, for this reason, the assumption on the density structure hardly affects the following consideration. We use the same profile as for the atmospheric analysis because the departures from LTE strongly influence the properties at the photospheric region where the polarization is produced.

Two different boundary conditions of the central emission will be investigated: (a) The emission corresponds to a surface of constant brightness (CS) and (b) the core emission is isotropic (IE). Obviously, this assumption (a) would result in a direction dependent luminosity at the core. This situation would occur if the diffusion time scale in the polar direction is lower than the one in the equatorial direction and it would be the realistic case if Thomson scattering controls the opacities at the inner layers. This is most reasonable for SN II.

Anticipating that the density slope and the radius are known from the atmospheric analysis, a specific configuration is characterized by the axis ratio E, the inclination i from which SN 1987A is seen and by the inner boundary condition. We will identify a configuration by its vector (E, i, boundary condition) in the following.

The observed spectra can be well reproduced by the atmospheric models and it may be attractive to use directly the density slopes, as it is generally done not only for supernovae but for different objects (Mendez et al. 1988; Jeffry 1987; Cassinelli et al. 1987). Since this treatment is appropriate for luminous SN II during the phase of density bounded photospheres (see below) we will discuss this in some detail. Keep in mind that this is misleading totally in the case of SN 1987A. For demonstration we refer to Fig. 8 where the results of some calculations for oblate and prolate ellipsoids are compared with the observations. The inclination i has been chosen such that the size of the polarization can be fitted best for the early times. The prolate ellipsoids with an isotropic emission show the correct time dependence and match. In contrast to the prolate ellipsoid with $E=1.2$ the oblate ellipsoids, produce a linear polarization which is slightly increasing with time and they can be ruled out for the explanation of SN 1987A. These slopes are caused by the decreasing depolarization by the extension of the envelope as a consequence of the flattening density slope. The increase is comparatively small (see Fig. 2) because the recombination prevents the envelope from further expansion. Although the same effect also works for the prolate geometry with IE, the polarization decreases at moderate optical depths for intermediate ellipsoids (see Fig. 5). The specific optical depth, at which the polarization shrinks, depends on the density slope and the non-isotropy of the global radiation field. This explains both the slope of the fitting configuration and also the difference between the two prolate structures which we have just investigated. One may then conclude that the envelope is axially elongated by about 10–20% and it is seen nearly equator on.

This result is based on the assumption that the electron profile can be represented by the density slope. Because the density slope at the photosphere decreases with time in the hydrogen rich envelope for SN II, the polarization can be expected to increase with time before the recombination phase. However, the density and electron profiles differ strongly after the recombination phase of hydrogen (Höflich 1990ab), and this approximation for the electron distribution is inadequate. Strong optical lines of heavy elements occurred in the spectra of SN 1987A already 1 to 2 weeks after the explosion of Sanduleak $-69°202$, indicating that for SN 1987A the recombination phase had been encountered. Consequently, the density and electron slopes were very different during the time of measurements of the polarization (see Table 1). The density slope of the electron density is represented by a smaller region with less influence on the emitted spectra. This implies less information to test the reliability of the slope at this region. Moreover, the absolute size of the polarization is smaller than in the density bounded phases and, consequently, larger errors have to be taken into account from the detections. Therefore, the earlier measurements should be given greater weight in determining the configuration.

For the polarization, the electron density slope at about $\tau = 1$ in Thomson scattering is relevant. For simplification and also for technical reasons, we have assumed power law profiles which correspond to the scale height of the electron concentration (see Table 1). The scale height decreases during the expansion of the envelope, i.e. the time dependence of the electron profile show the opposite tendency to that of the density profile. It should be kept in mind that the exponent $\tilde{n}_{el}$ may vary over the polarization forming region up to about 10%, although this hardly effects the results. It does not change the depolarization effect significantly.

The decrease of the polarization can be well understood as a consequence of the steepening electron density slope in the continuum forming region (see Figs. 9–10). Consequently, the polarization is increasing again after about day 30. This variation does not depend on the global geometry and it reflects the change of the photospheric parameters. However, it depends quantitatively on the inclination i and the specific geometry. The observations can be reproduced by oblate and prolate ellipsoids which either show IE or a CS at the core, and which were seen with different inclination i. The following basic data sets (E, i, emission type) are possible:

(a) (0.8, 44°, IE),
(b) (0.8, 56°, CS),
(c) (0.9, 5°, IE),
(d) (0.9, 40°, CS),
(e) (1.2, 0°, IE),
(f) (1.2, 30°, CS) and
(g) (1.1, 30°, CS).

A prolate ellipsoid with an isotropic emission and $E = 1.1$ can be excluded because it would not be able to produce the amount of polarization during very early phases.

The allowed ranges of i are about 5–10° depending on multiple scattering effects. Hence, a non-axi-symmetric configuration cannot be ruled out but can still produce some polarization. We can conclude that global deviations from sphericity slightly less than 10% up to 20% are consistent with the observations. The maximum eccentricity cannot be limited just on the basis of polarization measurements since even a very flattened ellipsoid shows a small polarization if it is seen nearly pole on. Even an axis ratio of 0.5 (see last section) cannot be ruled out on this basis. Therefore, we have to ask for some additional information from the observations which we have not yet used.

Up to now we have not paid attention to the direction dependence of the flux caused by the asymmetry if the envelope is optically thick for Thomson scattering. It provides some additional information about the deviations from sphericity which can be extracted from the observed bolometric LC. It allows us to deduce a limit of the deviations from sphericity for axial symmetric configurations. The difference between the mean and the direction dependent luminosity are given in the Figs. 9 and 10. Hence, the differences range up to 25% corresponding to a change of about 0.3^{mag} of the LC. The latter is well above the observational limits. The late LC of SN 1987A follows the linear decline of ^{56}Co up to about day 500 better than $0^m.1$, although the envelope becomes partially transparent in Thomson scattering after about day 300. Anticipating an axially symmetric geometry, the configuration (b) can be ruled out. All deviations from sphericity larger than about 20% do not agree with the LC. Conclusively, the most probable configurations have an inclination angle of about 30 . . . 40° and a flattening of about 10% and 20% for oblate and prolate ellipsoids, respectively. The fact that the direction dependent luminosity at $i = 30$–$40°$ matches the mean luminosity, is caused by the ellipsoidal geometry. Larger equatorial inclinations imply smaller deviations from sphericity. An inclination larger than about 56° does not allow for a simultaneous fit of the observed bolometric luminosity and the linear polarization because the two investigated boundary conditions may be regarded as the somehow extreme cases which bracket the possible range of real configurations (see above).

Table 1. The distance R_{ph} at which the optical depth is 1 for true absorption at 5000 Å, the effective temperature T_{eff}, the particle density N_0, the velocity field v in km s^{-1} and the mean value of $\tilde{n}$ corresponding to a density profile $N(r) \propto r^{-n}$ of the continuum forming region ($0.1 \leq \tau_{5000} \leq 1.0$) are given for the models (for the density profile see text). All quantities are given in cgs units. $\dot{M}$ is the mass in solar units which has gone through the photosphere, the radius $R_{H\,II}$ of the H II-region and the corresponding data are given for SN 1987A. The velocity v includes a statistical term of the order of 5 to 20%. In one column we give the density slope $\tilde{n}_W$ as resulted from the model 10H of Woosley et al. (1987). The last two values cannot be given because these regions would correspond already to the helium rich layers. In addition, we give the exponent $\tilde{n}_{el}$ which corresponds to the scale height of the electron density slope at the scattering optical depths of $\tau_{sc} \approx 1$ (from Höflich 1988a)

No.	R_{ph}	T_{eff}	N_0	v	$\tilde{n}$	$R_{H\,II}$	Date	$\dot{M}$	$\tilde{n}_W$	$\tilde{n}_{el}$
I[a]	$1.28\,10^{14}$	12400	$3.8\,10^{12}$	20000	13.0	—	Feb. 25	$7.0\,10^{-3}$	11.1	13
II[a]	$2.4\,10^{14}$	9150	$1.3\,10^{12}$	16500	10.0	$3.9\,10^{14}$	Feb. 26	$1.2\,10^{-2}$	9.5	10
III[a]	$4.9\,10^{14}$	6500	$4.8\,10^{11}$	12000	7.2	$7.8\,10^{14}$	Mar. 02	$2.5\,10^{-1}$	8.5	12
IV[a]	$8.5\,10^{14}$	5300	$3.6\,10^{11}$	8000	5.6	$1.15\,10^{15}$	Mar. 09	$8.0\,10^{-1}$	6.2	23
V	$1.07\,10^{15}$	5800	$2.7\,10^{11}$	4900	4.3	$1.25\,10^{15}$	Mar. 23	2.3	4.7	34
VI	$1.17\,10^{15}$	5900	$2.2\,10^{11}$	3300	2.8	$1.48\,10^{15}$	Apr. 16	5.2	3.0	26
VII	$1.21\,10^{15}$	6160	$2.0\,10^{11}$	1800	2.6	$1.58\,10^{15}$	May 14	7.1	2.4	20
VIII	$9.40\,10^{14}$	6300	$1.9\,10^{11}$	1100	2.2	$1.30\,10^{15}$	June 05	9.3	—	22
IX[b]	$7.8\,10^{14}$	4900	$1.5\,10^{11}$	800	1.9	$1.17\,10^{15}$	Oct. 02	11.7	—	18

[a] Pure hydrogen (and helium) model.
[b] Outer density structure is given by models I–VIII ($v_{stat} = 250$ km s^{-1}), excitation by γ rays.

5. Discussion and conclusion

For the understanding of the polarization, the importance of the optical depth effects, the occultation, and the size of the photospheric radius has been demonstrated in the first part. In particular, the observed polarization of scattering dominated photospheres of SN II can be expected to be very sensitive to the density slope in contrast to the optically thin approximation (Brown & McLean 1977). The direction dependence of the luminosity has been investigated in some detail and its implication on the observed LCs of SN II has been discussed.

In the case of SN 1987A the observed linear polarization in the continua is reanalysed. Anticipating an ellipsoidal density structure, the size of the deviations from sphericity could be limited to be less than 20% with an inclination angle i of less than 56° and a most probable value of about 30 to 40%. Both oblate and prolate ellipsoids are consistent with the time dependence of the observations which is caused by the raising electron slope because SN 1987A encountered the recombination phase very early. Keep in mind that the density profile and electron profile differ substantially at this stage. The upper limits of the inclination and the deviations from sphericity are both determined on the basis of the direction dependent luminosity and the observed LC.

In this respect the observation of Wampler et al. (1990) may be of high interest. They found the circumstellar matter to be axial elongated with an inclination angle which clearly excludes the polar and the equatorial viewing direction. Although the axis ratio of the wind of a blue supergiant certainly does not reflect the flattening, the symmetry axis should not be altered. Thus, this favours a moderate inclination, too.

Keep in mind that the observed bolometric LC of SN 1987A decays faster after about day 500 than implied by the ^{56}Co decay since a certain amount of the γ radiation can escape freely. For this reason, more detailed light curve calculations may permit a further improvement of the limits for the axis ratio and, in particular, for i.

As we have seen, an inclination angle of more than 56° is hardly compatible with the observations. On the other hand, Janka & Mönchmeyer (1988) have concluded from the observed neutrino signal by IMB and Kamikande that the progenitor was probably seen at larger i providing a rapidly rotating core. From the previous study, one may conclude that this was not the case. However, this question needs further investigation because of its strong implications for the mechanism which causes the explosion (Hillebrandt & Höflich 1989; Fryxell et al. 1990).

It may be of interest for the future observations of SN II besides SN 1987A that the polarization is to be expected at maximum for oblate ellipsoids just before the recombination phase, i.e. before strong lines in the optical wavelength occur (see Fig. 8).

Finally, we want to mention the limits of this investigation. First, axially symmetry has been adopted. It must be expected that also small scale structures may result in some polarization if their number remains small or if the small scale structures have a certain orientation. Furthermore, although the assumption of pure scattering is a good approximation, the incorporation of absorption processes may be helpful to distinguish between the cases of isotropic emission and a surface of constant brightness and it might improve quantitatively the results.

References

Arnett W.D., Bahcall J.N., Kirshner R.P., Woosley S.E., 1990, ARA&A 27, 629

Barrett P., 1987, in: SN 1987A, ed. I.J. Danziger, ESO, Garching, p. 173

Brown J.C., McLean I.S., 1977, A&A 57, 141

Arnett W.D., Bahcall J.N., Kirshner R.P., Woosley S.E., 1990, ARA&A 27, 629

Cassinelli J.P., Nordsiek K.H., Murison M.A., 1987, ApJ 317, 290

Catchpole R.M., Menzies J.W., Monk A.S., Wargau W.F., Pollacco D., Carter B.S., Whitelock P.A., Marang F., Laney C.D., Balona L.A., Feast M.W., Lloyd Evans T.H.H., Sekiguchi K., Laing J.D., Kilkenny D.M., Spencer Jones J., Roberts G., Cousins A.W.J., van Vuuren G., Winkler H., 1987, MNRAS 229, 15

Clayton G.C., Martin P.G., Thompson I., 1983, ApJ 265, 194

Colcciatti A., Mendez M., Benvenuto O., Feinstein C., Marraco H., Garcia B., Morrell N., 1988, Proc. of the 4th George Mason Conference on SN 1987A, eds. M. Kafatos, A. Michalitisianos, Cambridge University Press, Cambridge, p. 70

Daniel J.Y., 1982, A&A 86, 198

Hillebrandt W., Höflich P., 1989, Reports in Prog. in Phys. 52, 1421

Höflich P., 1988a, Proc. Astron. Soc. Aust. 7, 434

Höflich P., 1988b, IAU Symposium 108: "Atmospheric Diagnostic of Stellar Evolution", ed. K. Nomoto. Springer, Berlin Heidelberg New York, p. 388

Höflich P., 1990a, Supernovae, ed. Woosley, Springer, Berlin Heidelberg New York, p. 415

Höflich P., 1990b, Analysis of type II supernovae at the photospheric phase, Munich, habilitation thesis

Höflich P., Sharp Ch.M., Zorec J., 1989, Particle Astrophysics Workshop Berkley, ed. E.B. Norman, World Scientific, Singapure, p. 186

Janka H.-T., Mönchmeyer R., 1988, A&A 209, L5

Jeffry D.J., 1987, Nat 329, 419

Mendez M., Clocchaiatti A., Benvenuto G., Feinstein C., Marraco U.G., 1988, ApJ 334, 295

Schmidt Th., 1976, A&AS 24, 357

Schwarz H.E., 1987, in: SN 1987A, ed. I.J. Danziger, ESO, Garching, p. 167

Schwarz H.E., Mundt R., 1987, A&A 177, L4

Serkowski K., Mathewson D.S., Ford V.L., 1975, ApJ 196, 261

Shigeyama T., Nomoto K., Hashimoto M., 1988, A&A 196, 141

Symbalisty E.M.D., 1984, ApJ 285, 729

Van de Hulst H.C., 1957, Light scattering by small particles, Wiley, New York

Wampler E.J., Wang L., Baade D., Banse K., D'Odorico S., Gouiffes C., Tarenghi M., 1990, A study of the nebulosities near SN 1987A (preprint)

Weiss A., Hillebrandt W., Truran J.W., 1989, A&A 197, 111

Woosley S.E., 1988a, ApJ 330, 218

Woosley S.A., Pinto P.A., Ensman L., 1987a, ApJ 324, 664

Yamada S., Sato K., 1990, ApJ 358, L9